LA-UR 88-2533

Los Alamos National Laboratory is operated by the University of California for the United States Department of Energy under contract W-7405-ENG-36.

TITLE: MK-82 BOMB CHARACTERIZATION FOR THE SYMPATHETIC DETONATION STUDY

AUTHOR(S): Roy A. Lucht and Lawrence W. Hantel

SUBMITTED TO: Twenty-Third DoD Explosives Safety Seminar
August 9-11, 1988
Atlanta, Georgia

Los Alamos
Los Alamos National Laboratory
Los Alamos, New Mexico 87545

FORM NO. 836 R4
ST. NO. 2629 5/81

MK-82 BOMB CHARACTERIZATION for the SYMPATHETIC DETONATION STUDY

by

Roy A. Lucht
and
Lawrence W. Hantel

ABSTRACT

Optical, radiographic, and electronic pin techniques were used to evaluate the fragmentation of tail- and side-initiated MK-82 MOD 1 general purpose bombs. They were found to contain large voids, randomly located from bomb to bomb, in the Tritonal explosive fill. Characteristics of the void-side performance of the bomb were found to be as much as 10% different from the nonvoid side and were much less reproducible than the characteristics of the nonvoid side. The data collected will be useful in evaluating sympathetic detonation mitigation systems designed for use with the bombs.

I. INTRODUCTION

The U.S. Air Force is involved in an insensitive munitions study, part of which includes an assessment of how to prevent sympathetic detonation of stored conventional munitions by means of mechanical suppressants. The Los Alamos National Laboratory has been participating in this effort since FY1986 with funds provided by AD/XR-3, Eglin Air Force Base, Florida.

The Los Alamos approach to the problem of sympathetic detonation is different from the traditional approach. Traditionally, large-scale tests of bomb arrays are conducted to statistically determine the efficacy of the proposed solution. However, if 20 or more bombs are involved in each test, the cost per test eliminates the possibility of large-number statistics. In addition, because of the threshold nature of the sympathetic detonation problem, we cannot infer that several successful large-scale tests will eliminate the possibility of future system failure. In sympathetic detonation testing, as with all explosives sensitivity testing, there is a region of input stimulus over which either a detonation or no reaction may occur. The simple case of explosive detonation caused by fragment impact is illustrated schematically in Fig. 1. A fragment with velocity in the range of v_1 to v_2 may or may not cause detonation on any given experiment. If the velocity is below v_1, detonations do not occur and if it is above v_2, they always occur. A small number of large-scale tests cannot be used effectively to calibrate such effects. The Los Alamos approach is to determine threshold values for detonation from various stimuli, then mitigation

schemes can be evaluated as to their ability to reduce the input stimuli to well below the threshold values.

Sympathetic detonation can be caused by a number of processes including fragment impact, shock transmission through a physical suppression system, or heating caused by physical distortion of acceptor bombs. As a first step to evaluating sympathetic detonation of MK-82 systems, we will characterize the donor to determine the worst-case fragments, shock strengths, etc. The second step is to determine acceptor thresholds for detonation, and the third step is to design and evaluate mitigation schemes for their capability to reduce the output to values well below the acceptor threshold levels. In this paper, we report the MK-82 donor characteristics of fragments close to the bomb, where they could be expected to affect acceptor bomb response.

II. EXPERIMENTAL RESULTS

MK-82 bombs contain about 87 kg of Tritonal explosive (80 wt% TNT/20 wt% Al). It is not an ideal system to characterize, from an explosives viewpoint, because the cast Tritonal fill is not homogeneous and contains large shrinkage voids. A typical void occupies 3 to 5% of the explosive cross section and is lined by TNT crystals. The void was generally within 10 to 25 mm of the bomb case. To characterize donor output, it was important to know where the void area was and to measure what effect it might have on fragment characteristics, as compared with those produced on the nonvoid side.

Because we needed to establish the void location for each shot, every MK-82 bomb was radiographed before being fired. Orthogonal views were taken to precisely determine the void location with respect to lifting lugs. The void side of the bomb was then oriented appropriately for each shot.

Three series of experiments have been completed. The first series consisted of tail-initiated bombs, in which tests, the primary diagnostic technique was radiography. The second series used tail-initiated bombs with streak and image intensifier cameras. The third series used side-initiated bombs and radiography. Electronic pins were used on all shots. For the tail-initiated bombs, the fuze well was packed with 125 mm of Composition C. A detonator and a booster were used to detonate the Composition C on the bomb axis. For the side-initiated bombs, a 50-mm-long by 50-mm-diameter cylinder of HMX-based explosive was pressed onto the side of the bomb with a thin layer of PETN-based soft explosive used to fill in the area between the flat explosive cylinder face and the curving case.

A typical shot setup for the first series of experiments is shown in Fig. 2. At the far right, behind the sandbags, are the x-ray heads that operate remotely from the Marx banks (beyond the picture). The sandbox to the right center protects the x-ray heads and holds lead shades used to separate the two beams. The bomb is in the center, laying on a wooden table well below ground level. It is surrounded by sandboxes to protect equipment from fragments. At the far left are the film cassettes. A sheet of Plexiglas is placed at a 45° angle to the

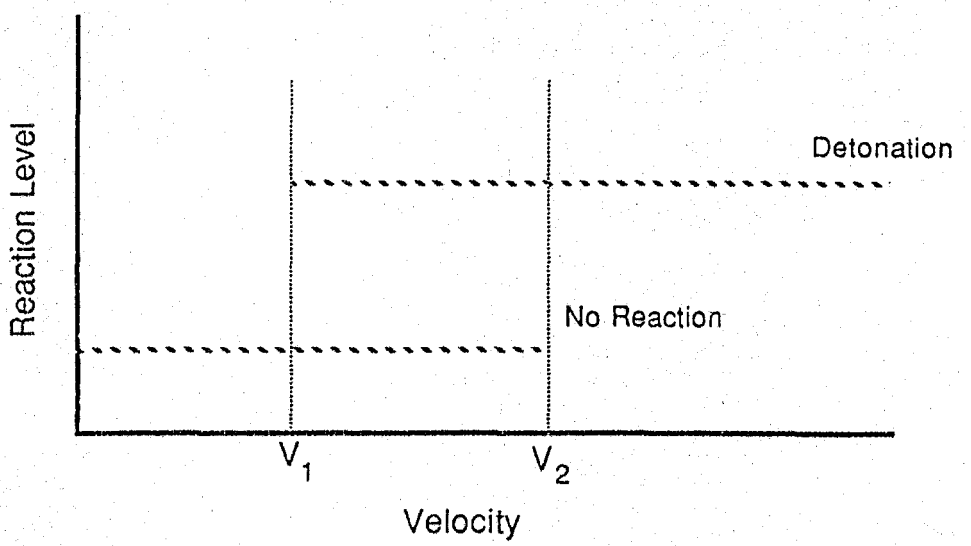

Fig. 1. Explosive reaction level versus fragment impact velocity for typical fragment impact sensitivity test.

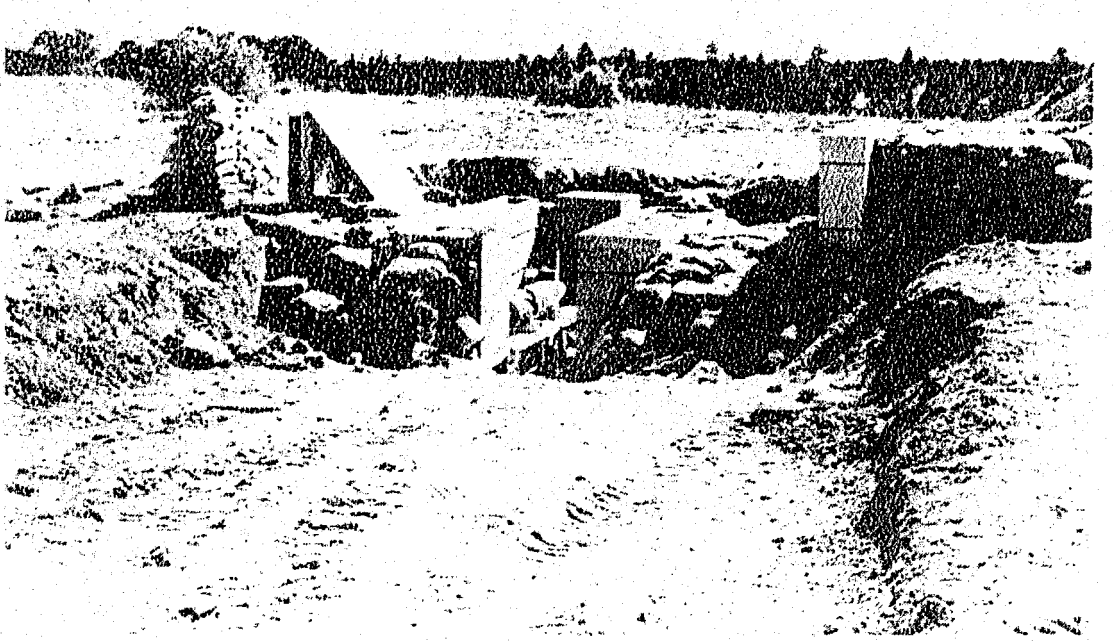

Fig. 2. Typical shot setup for MK-82 bomb characterization study.

cassettes to deflect the blast wave. The sandbags behind the cassettes slow them after they are launched by the bomb blast.

We were interested in early bomb-case motion to verify that the bomb detonated high order and to see if the initial motion was different on the void and nonvoid sides. Linear electronic-pin arrays were used to record a phase velocity down the bomb axis. These pins were located in a straight line on the outside surface of the bomb case at known distances from the tail. When the case started to move because of the shock driven by the detonation wave, the pins shorted out and produced timing signals. These arrays gave phase velocities in excess of Tritonal detonation velocity (6.5 mm/μs), which means that in each case the bomb detonated high order. The velocities were determined from least squares fits to the distance/time data as shown for Shot R0643 in Fig. 3.

Because some data sets contained only three or four data points, improved signal-to-noise ratio was achieved by combining like data sets and calculating least squares fits. The results for the nonvoid and void sides are shown in Figs. 4 and 5, respectively. Circled data points were not included in the fits. A statistically real difference in the two sides is evident. The phase velocity is 1% slower on the void side and the wave on the void side is delayed 4 μs at 150 μs, with respect to the wave on the nonvoid side. Although these differences are real, they are too small to be considered a significant difference in bomb performance.

Hexagonal electronic capped-pin arrays were used on Shots R0646 and R0647 to record the first few centimeters of bomb case expansion. Seven capped pins were mounted in a Plexiglas block in a centered-hexagonal configuration with 12.7 mm being the maximum distance between pin axes. The pins in an array were staggered radially out from the bomb case with the first pin touching the case and the last pin about 64 mm away. As the case accelerates radially out, the pins are successively shorted, giving a distance/time profile. Three arrays were used on Shot R0646, all located 635 mm from the bomb tail and at 90° intervals around the bomb (one over the void area, one 90° around the bomb, and the third 180° from the void). For Shot R0647, two arrays were located 635 mm from the bomb tail: one over the void area and the other 180° away. The third array was located over the void but an additional 119 mm down the bomb axis.

Figure 6 shows all data from the six arrays. The nonvoid data from both shots are nearly identical, whereas the void data lie on both sides of the nonvoid data. This points out the early motion shot-to-shot reproducibility problem created by the inhomogeneous explosive fill. These early case motion data provoked us to attempt several cylinder tests with the MK-82 bomb. Shots C5973 and C5977 produced excellent data. A smear camera and an image intensifier camera array were used on both shots to evaluate case motion optically, simultaneously on the void and nonvoid sides of the same bomb. Smear camera data from Shot C5973 are shown in Fig. 7 and image intensifier camera data from Shot C5977 are shown in Fig. 8.

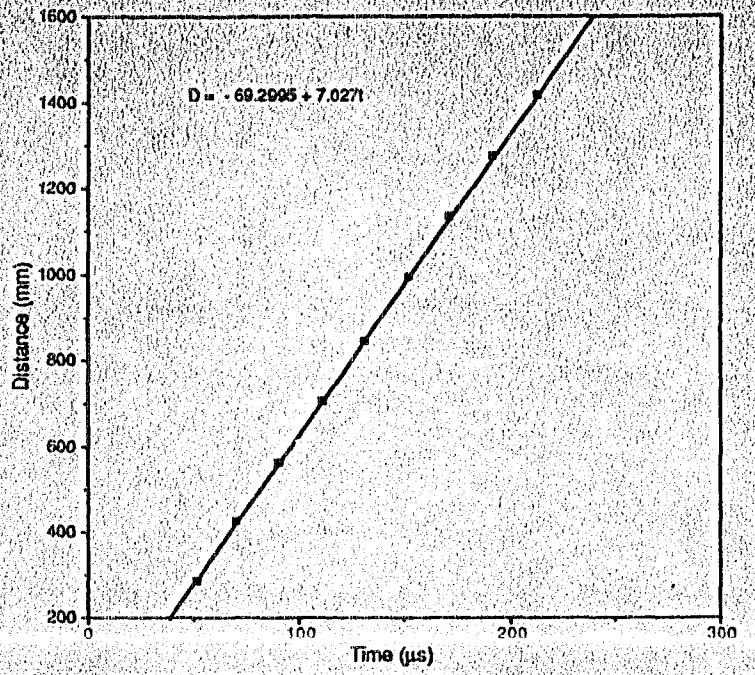

Fig. 3. Distance/time data for nonvoid case expansion, Shot R0643.

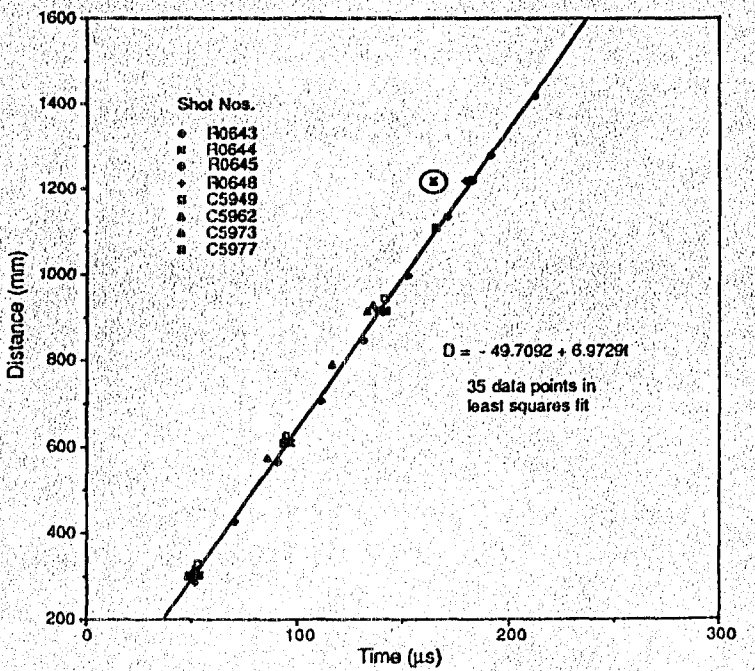

Fig. 4. All distance/time data for nonvoid case expansion.

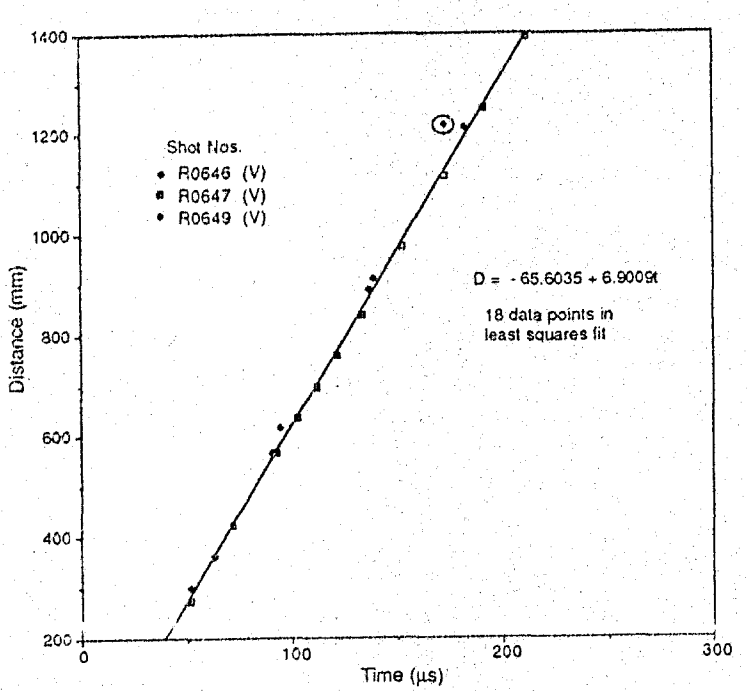

Fig. 5. All distance/time data for void case expansion.

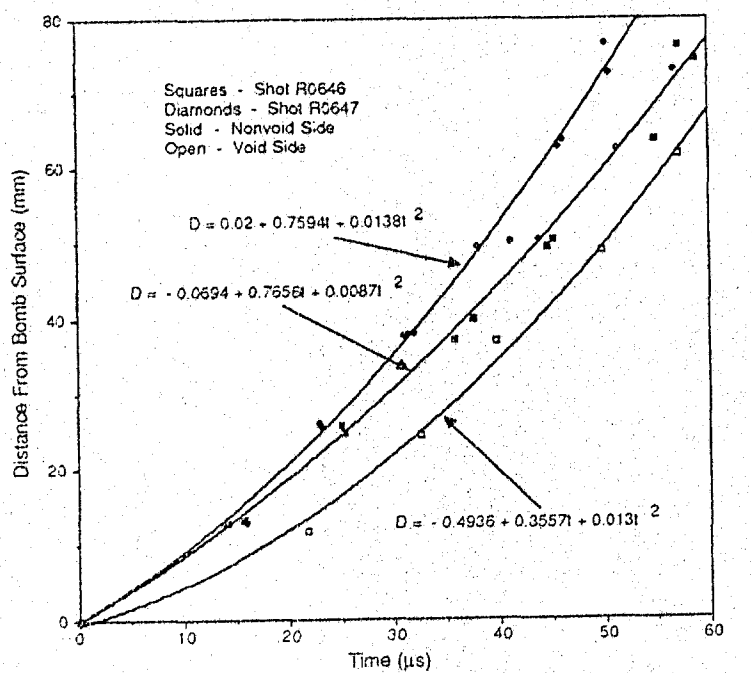

Fig. 6. Data from six capped-pin arrays, Shots R0646 and R0647.

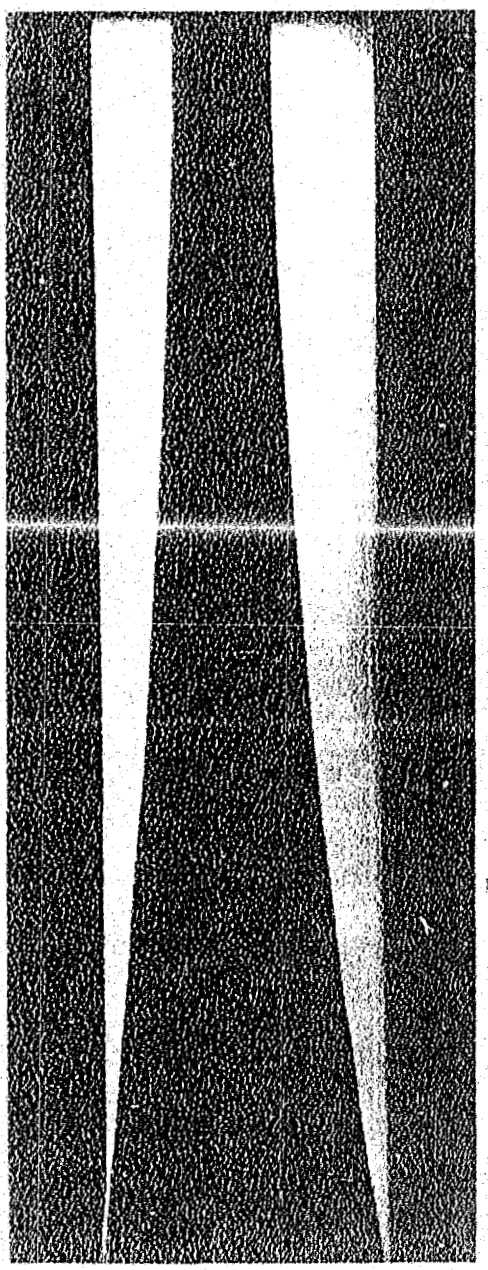

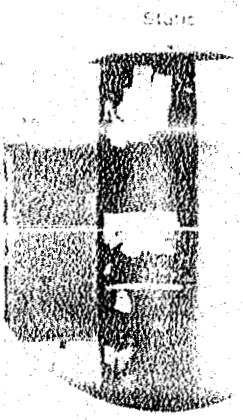

Fig. 7. Smear camera record for MK-82 void- and nonvoid-wall expansions, (Shot C5973). The slit is 635 mm from the bomb tail with the nonvoid side on the left and the void side on the right.

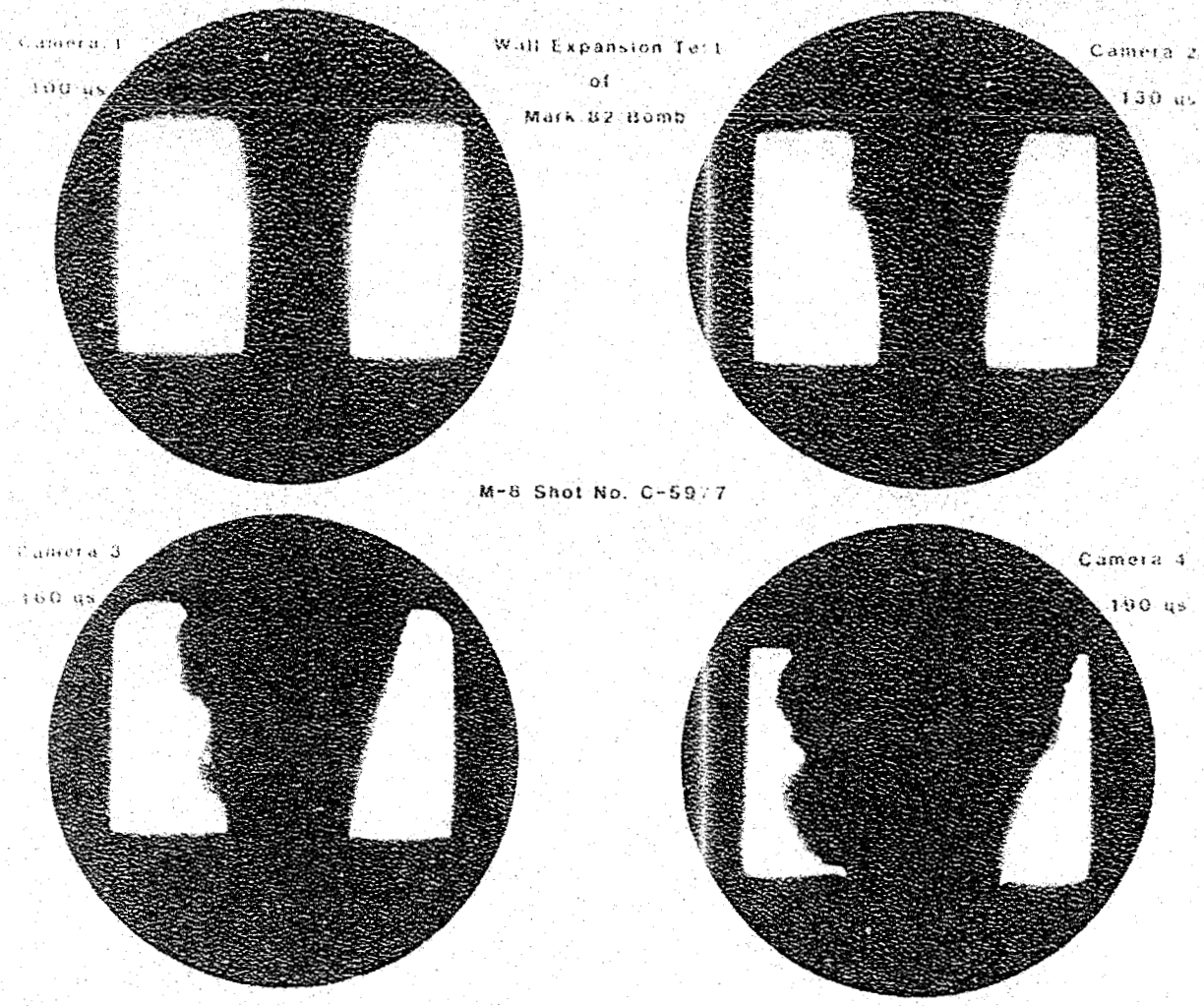

Fig. 8. Image intensifier photographs of MK-82 wall expansion (Shot C5977). The nonvoid side is on the left and the void side is on the right.

intensifier frames were also used to determine time and axial positions where the case ruptured. The fragmentation positions and times were highly variable. The only conclusion that can be drawn is that fragmentation is highly variable from point to point on a given bomb and does not correlate well with void position. This conclusion is also indicated by the large variety of fragment sizes and shapes observed in the flash radiographs. Fragmentation effects may be dictated more by random flaws in the steel case than by physical processes in the explosive. Also, once the case breaks at a given point, adjacent case material is subjected to radically different stresses; thus adjacent case pieces can fragment at very different radial expansion positions.

Good dynamic radiographs were obtained from five tail-initiated shots. Two dynamic radiographs were taken of each shot; the first one was taken several hundred microseconds after the detonator in the bomb tail was fired, and the second one, a hundred or so microseconds later. The times were chosen so that the radiographs were taken after the bomb case was completely fragmented and the maximum fragment velocity obtained. The two radiographs allowed us to record the bomb fragments at two distinct times and displacements, from which the fragments' velocities could be determined. Careful geometric measurements and still radiographs with fiducials provided crosschecked position references for the dynamic radiographs.

Figure 10 is an example of the dynamic radiographs (Shot R0649), and Table 1 lists the data measured from the radiographs. Because the fragments are from an expanding cylinder, only the leading fragments radiographed can be assumed to have a low- or zero- "Z" velocity component. In this Cartesian coordinate system, the "X" and "Y" components define a vertical plane above the bomb, where "X" is parallel to the bomb axis, "Y" is vertical, and "Z" is parallel to the direction of the x-ray beam propagation. Thus, for the radiograph to be useful, it is mandatory that leading-edge fragments can be identified in both exposures. Because the fragments are irregularly shaped and tumbling, the cross-sectional areas can be considerably different at the two times viewed in the experiment. The area values indicate the visible range of sizes, showing no obvious large difference between the observed fragments from the void and nonvoid sides.

The radiographic analyses for all the shots included some very small, fast particles, and some particles well below the leading edge, where they may have significant "Z" component velocities that cannot be resolved. To compare void- and nonvoid-side performances, only fragments representing large leading-edge fragment motion should be considered. Because they are large, these fragments represent the bomb case motion best and have the most consistent velocities. Thus, an analysis was performed in which the large leading-edge fragments were chosen without regard to their velocities, from all experiments, and their velocities averaged. The averages included 8 fragments for the void side and 19 for the nonvoid side. The results are

$V = 2.215 \pm 0.005$ mm/μs, void, and;
$V = 1.947 \pm 0.018$ mm/μs, nonvoid.

Streak camera data can best be displayed on distance/time plots. This is done for the two most successful shots in Fig. 9. Also displayed in Fig. 9 are all the hexagonal capped-pin array data. For all early case motion data taken, all nonvoid-side data were consistent. All void-side data were also consistent (with somewhat larger scatter) with the exception of the data of Shot R0647, which fell above the nonvoid data. All other void-side data fell below the nonvoid-side data. Because the location and size of the void are so nonreproducible, void-side expansion can be expected to vary greatly from bomb to bomb and from spot to spot for a given bomb.

The physical processes creating the pressure that drives the bomb case may be considerably different for the void and nonvoid sides. One hypothesis is that the detonation wave is fully supported and creates a high pressure at the steel case as it passes. This high pressure is maintained by the large bulk of explosive behind the steel and drives the steel at an initially high acceleration. The acceleration drops slowly but continuously as the expansion of the detonation products proceeds and the pressure drops correspondingly. On the void side, the initially high acceleration should be short lived because the gaseous detonation products can expand into the void, dropping the pressure. Case expansion then proceeds at a slower rate for a while. The products expanding into the void will collide with products from explosive from the other side of the void (the center of the bomb), causing the wave to reflect and the pressure to increase greatly. This high-pressure region then expands and catches up to the case, causing significant late-time acceleration. This is precisely the behavior seen in the data. All the data (except void-side data from R0647) show void and nonvoid-side expansion overlapping (i.e., identical acceleration) for about the first 5 μs. Then the nonvoid side case moves ahead of the void-side case until about 40 μs. Around 40 μs (depending on the void geometry of the given shot), the void-side case experiences higher acceleration than the nonvoid-side case and eventually passes it up. Evidence for this is seen in the higher fragment velocities measured from the flash radiographs discussed later in this paper. The x-t trajectories of the void- and nonvoid-side cases must cross shortly after fragmentation occurs but out of the smear camera view. If the first derivatives are taken of the least squares fits, velocities can be calculated at 80 μs. Fragmentation has usually occurred by 80 μs, and this is about the limit of where the least squares fit can be trusted. This was done yielding the following average velocities:

$$V(80\ \mu s) = 2.14\ mm/\mu s, \quad \text{void;}$$
$$V(80\ \mu s) = 1.92\ mm/\mu s, \quad \text{nonvoid.}$$

The difference in velocities is about 10%, which agrees well with the velocities obtained from the radiographic data. The fragment velocities from the radiographic data are slightly higher than these, which is understandable because some positive acceleration can be expected even after the case fragments. Acceleration stops or becomes negative only after the detonation products pass the fragments and produce equal pressure on all sides.

The streak camera data could also be used to determine when the case ruptured at the slit position (635 mm from the tail). Several of the image

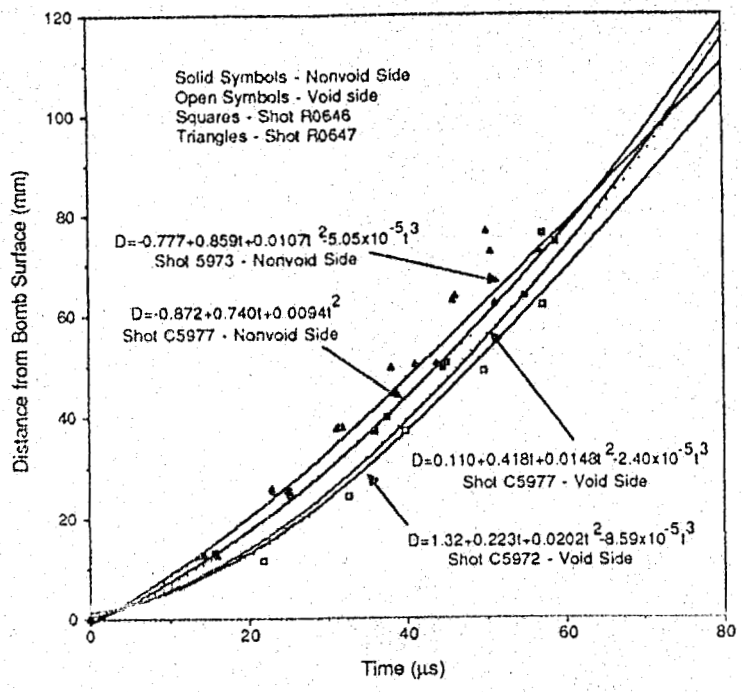

Fig. 9. Distance/time data from smear camera Shots C5973 and C5977 and from capped-pin array Shots R0646 and R0647.

Fig. 10. Dynamic radiographs of MK-82 bomb fragments from nonvoid side (Shot R0649). Bottom radiograph at 631 μs; top one at 727 μs.

TABLE I

FRAGMENT AREAS, VELOCITIES, AND ANGLES FOR SHOT R0649

Fragment Number	Film I Area (cm^2)	Film II Area (cm^2)	V(x) (mm/μs)	V(y) (mm/μs)	V (mm/μs)	Ø (degrees)
1	21.50	21.68	0.25	2.09	2.11	6.80
2	9.19	7.86	0.06	2.17	2.17	1.67
3	5.27	3.35[a]	0.24	1.96	1.97	6.96
4	3.36	2.70	0.29	1.71	1.73	9.55
5	3.20	5.51	0.38	1.85	1.88	10.96
6	6.44[b]	4.42[b]	0.26	1.82	1.84	7.98
7	6.46[b]	6.72[b]	0.50	1.97	2.04	14.18
8	12.56[a]	13.72	0.22	2.21	2.22	5.64
9	0.71	0.89	0.37	2.05	2.09	10.08
10	3.22	5.20	0.24	1.85	1.86	7.33
11	2.23	3.43	0.14	1.84	1.85	4.34

[a] Off edge of film.

[b] Long-fragment, arbitrary cutoff point.

V(av) = 1.98 ± 0.156 mm/μs

Ø(av) = 7.77 ± 3.392 °

Even if velocities two standard deviations closer are considered, the void-side fragments still have velocities at least 10% larger than nonvoid-side fragments. This agrees well with the streak camera data described above. Although this is statistically accurate, the difference is not large enough to be a major consideration when suppressant systems are designed, because velocities should be decreased much more than 10% below threshold levels.

Six side-initiated shots have been fired. Shot setup was almost identical to that shown in Fig. 2 for the tail-initiated shots except for the initiation scheme. A high-explosive cylinder (booster) was placed at the center of the bomb axially and on the side facing down (bottom of a bomb lying horizontally). For two of these shots, the voids were at the top of the bomb; for three, the voids were positioned to one side, and for one shot, the voids were at the bottom. In all experiments, linear pin arrays were used. Each array was positioned on a side of the bomb parallel to the bomb axis. Three or four linear arrays were used in each experiment. For reference, pin angles are measured from the bomb axis with vertical up being zero. Thus, pins that ran along the bottom are referred to as 180° data, along the side (in a horizontal plane through the bomb axis) as 90° data, and near the top of the bomb as 20° to 35° data. Pins could not be placed along the top (0°), because they might interfere with the radiographic analysis. Straight-line distances through the explosive between the explosive-bomb case interface above the booster (180° and axial center) and each pin (any angle and axial distance) were calculated and plotted versus pin arrival times. Good pin data were obtained for every shot. From

these data, detonation velocity and detonation wave corner-turning effects could be determined.

The linear pin array data were plotted for each array for all six experiments and linear least squares fits were calculated. The slopes of the lines correspond to wave velocities, most of which agree well with Tritonal detonation velocity. For Shot R0663, the void area was at the bottom of the bomb, adjacent to the detonation center. This shot failed to detonate, and the pin data showed the wave dying out away from the initiation point. This failure was probably caused by the layer of explosive between the bomb case and the void being too thin to sustain a detonation.

One linear pin array on each bomb ran along the bottom of the bomb (180° data) past the detonation center. For this configuration, the detonation wave must turn through essentially 90° before the data can be expected to show detonation velocity. Thus, the first several points can be expected to be slow and show significant scatter. This is just what is observed. If only the last several points are considered, the wave has had sufficient time to turn the corner and come up to detonation velocity.

A summary of the slopes from linear pin arrays for all side initiated bombs show considerable scatter; however, trends are obvious. In general, waves that do not pass through a void have a velocity near the measured Tritonal velocity. Waves that do pass through or near a void appear to be faster. Limited core samples of a bomb yield significantly varying aluminum concentrations in the Tritonal. Specifically, some of the explosive near the void appears to be almost pure TNT. A detonation wave passing through a region of low aluminum concentration will be considerably faster than one through a region of high aluminum concentration, because the TNT velocity is 7% faster than Tritonal velocity.

Note that these determinations of velocity are different than the standard rate stick experimental technique. With the rate stick method, times of wave arrival are measured at different points along a straight line. Here, each distance-time data point represents a different wave direction. Considering this, these data are remarkably linear.

A typical statistical technique to increase signal-to-noise ratio is to combine like data sets. The difficulty here is due to changing reference times. Reference times can change from experiment to experiment and from array to array for a variety of reasons. The detonator cables for this experiment are about 300 ft long, and ring-up time can shift. The thickness of the soft explosive used and its contact with the bomb case can change from experiment to experiment. These and other system variations would normally amount to less than one or two microseconds' difference. The main cause of changing reference times is believed to be bomb-to-bomb variability, variations in explosive composition within a bomb, and whether or not the wave passes near or through a void.

A good time to use as a reference for comparisons is the time from each linear least squares fit at which the distance (x) is zero. This can be viewed as a

starting time (i.e., delay time) for each wave corresponding to a single data set. These intercept times were averaged for each group of like data sets (90° data adjacent to a nonvoid side), and each data set was then shifted a constant time interval so that its new intercept was equal to the average. Least squares fits were then calculated for the entire group of data. An example is shown in Fig. 11. A summary of all the side-initiated pin data follows in Table II.

TABLE II

SIDE-INITIATED PIN DATA

Configuration	Number of Data Points	X=0 Intercept (μs)	Velocity (mm/μs)
35° nonvoid	22	22.4	6.248
20-35° void	16	21.0	6.600
90° nonvoid	28	23.3	6.534
90° void	22	30.8	6.717
180° nonvoid	19	26.3	6.549
180° void	detonation failed		

There were 38 data points available for the 180° nonvoid case; however, only the latest 19 were used to allow the detonation to come up to speed, as shown in Fig. 12. The time required to attain detonation velocity explains the large x intercept for this configuration. The only other anomalously large intercept is for the 90° void case and may correspond to an induction time for passing through or around the void. However, this is contradictory to the higher observed velocity for this case. A similar result is not observed for the 20-35° void case probably because, at these angles, the wave only grazes the void area. All velocities appear reasonable, although the velocity for the 35° nonvoid case is smaller than expected.

Useful radiographs were obtained on four side-initiated experiments: two with the voids up (voids at 0° position) and two with the voids on the side (90° position). The data were analyzed in the same way as those for the tail-initiated experiments. After fragment velocities and areas were determined, leading-edge fragments were selected and their velocities and areas were averaged for each experiment and for the two types of experiments giving the results in Table III.

R0662 is difficult to interpret because almost all of both dynamic radiographs are covered with fragments; thus it is impossible to prove that the top fragments are leading fragments and that no fragments were above the radiographs. If this were the case, then the average velocity of 1.91 mm/μs would be a lower bound. Even with this caveat, the void-side fragment velocities are at least 10% higher than the nonvoid-side fragments. This is essentially the same result as the tail-initiated series.

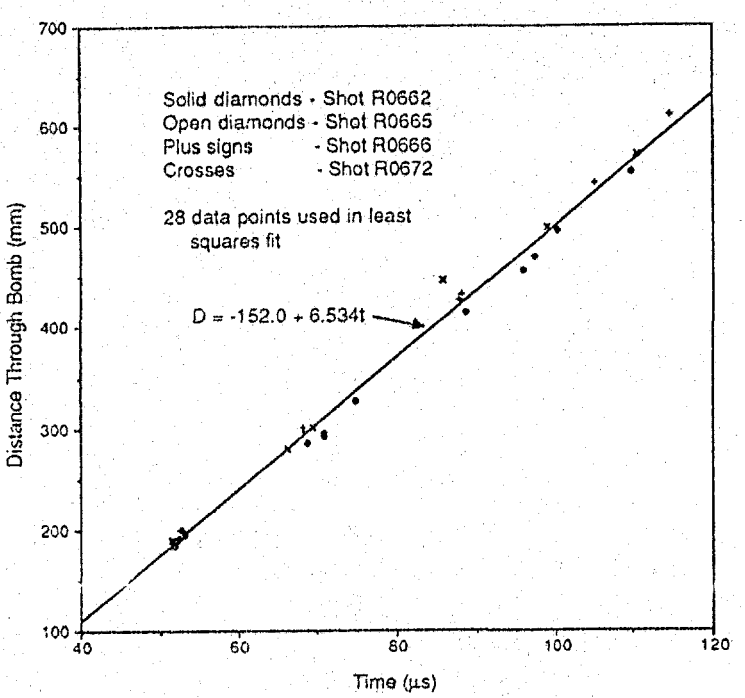

Fig. 11. Data from four linear pin arrays at 90° to the vertical on a nonvoid side, Shots R0662, R0665, R0666, and R0672.

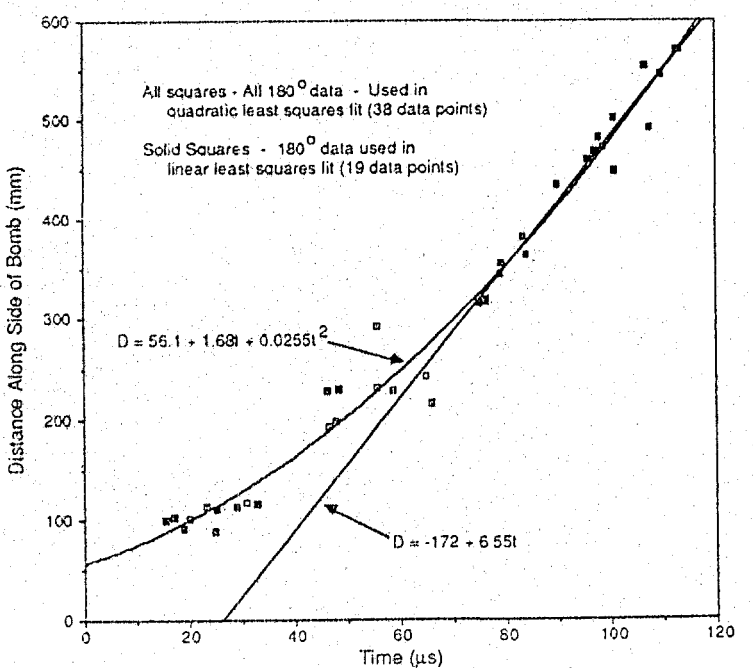

Fig. 12. Data from all side-initiated shots at 180° to the vertical (bottom of bomb), nonvoid side.

TABLE III

LEADING-EDGE FRAGMENT DATA

Experiment	Velocity (mm/μs)	Area (cm^2)	Number of Fragments	Configuration
R0662	1.91± 0.25	1.51 ± 1.07	8	Void Up
R0665	1.87 ± 0.11	2.86 ± 1.28	3	Nonvoid Up
R0666	1.85 ± 0.12	6.17 ± 2.59	6	Nonvoid Up
R0672	2.23 ± 0.28	2.82 ± 2.09	9	Void Up
R0662&R0672	2.08 ± 0.31	2.21 ± 1.80	17	Void Up
R0665&R0666	1.86 ± 0.11	6.06 ± 2.72	9	Nonvoid Up

Fragment sizes are more difficult to evaluate, because only areas of well-defined isolated fragments were measured, whereas areas of fragments in clusters could not be measured. Thus any conclusions made from averages of measured fragment areas are subject to question. The general impression after viewing the radiographs is that fragment sizes for the tail-initiated case were about the same size for the void and nonvoid sides; however, for the side-initiated case, the nonvoid-side fragments are about twice the size of the void-side fragments. The major difference in the experiments is that for the tail-initiated case, the detonation wave propagation vector is basically parallel to the bomb case; whereas, for the side-initiated case, it is orthogonal at the center and moves toward parallel at the ends of the bomb. Why the case should be more severely shattered in the void-side-initiated case is unknown; however, it may be due to collision of waves traveling in opposite directions in the thin section of Tritonal between the case and the void. Also, a subjective survey of the radiographs shows a larger variety of fragment sizes and velocities for the side-initiated cases than was observed for the tail-initiated bombs.This is reasonable because orthogonal waves often cause a plate to spall as well as fragment.

III. CONCLUSIONS

Statistically significant differences were observed in the behavior of the void side of the bomb compared with the nonvoid side for both tail- and side-initiated MK-82 bombs. In addition, differences were observed in the initial acceleration of the bomb case, which could result in different pressures being transmitted into close objects such as material intended to mitigate sympathetic detonation. Although average differences in fragment velocity of at least 10% were observed, individual high-velocity fragments can be generated from either the void or nonvoid sides. A nonstatistical survey of the fragment data indicates that only a few fragments with areas of a few square centimeters have velocities above 2.4 mm/μs. Thus if a suppressant system can be developed that reduces the velocities of these fragments to below the initiation threshold, a fragment-induced sympathetic detonation should not propagate through a stack of bombs.

ACKNOWLEDGMENTS

Many scientists and technicians contributed to this work, and the major contributors are listed here. Richard Garcia was firing-site leader for the flash-radiography experiments. He was assisted by Walter Quintana and Max Avila. Dan Hughes was firing-site leader for the streak camera experiments and was assisted by Tommy Herrera and Ken Uher. Jerry Langner analyzed the radiographs for fragment velocity and size, and Warner Miller read the streak and image intensifier films and produced position-time data from them.